Published in final edited form as:
Microvasc Res. 2011 November ; 82(3): 385–390. doi:10.1016/j.mvr.2011.06.009.

Retinal transfer of nicotinate by H+-monocarboxylate transporter at the inner blood-retinal barrier

Masanori Tachikawa[1,2], **Koji Murakami**[1], **Pamela Martin**[2], **Ken-ichi Hosoya**[1], and **Vadivel Ganapathy**[2]

[1]Department of Pharmaceutics, Graduate School of Medicine and Pharmaceutical Sciences, University of Toyama, Toyama, Japan

[2]Department of Biochemistry and Molecular Biology, Medical College of Georgia, Georgia Health Sciences University, Augusta, Georgia, USA

Abstract

Nicotinic acid is a constituent of the coenzymes NAD and NADP. It also serves as an agonist for the G-protein-coupled receptor GPR109A. Nicotinic acid is widely used at high doses as a lipid-lowering drug, which is associated with an ocular side effect known as niacin maculopathy. Here we investigated the mechanism by which nicotinate is transferred into retina across the inner blood-retinal barrier (BRB). *In vivo* the blood-to-retina transport of [^{3}H]-nicotinate was studied using the carotid artery injection technique. The characteristics of nicotinate transport at the inner BRB were examined in a conditionally immortalized rat retinal capillary endothelial cell line (TR-iBRB2), an *in vitro* model of inner BRB. The expression of transporters in TR-iBRB2 cells was determined by reverse transcription-polymerase chain reaction. *In vivo* [^{3}H]-nicotinate uptake by the retina was 5.4-fold greater than that of [^{14}C]-sucrose, a BRB impermeable vascular space marker. Excess amounts of unlabeled nicotinate and salicylate significantly decreased the *in vivo* retinal uptake of [^{3}H]-nicotinate. [^{3}H]-Nicotinate was taken up by TR-iBRB2 cells via an H^+-dependent saturable process with a Michaelis constant of ~7 mM. Na^+ had minimal effect on the uptake. The H^+-dependent uptake was significantly inhibited by endogenous monocarboxylates such as lactate and puruvate, and monocarboxylic drugs such as valproate, salicylate, and ibuprofen. These characteristics are consistent with those of H^+-coupled monocarboxylate transporters (MCTs). MCT1, MCT2, and MCT4 mRNAs were expressed in TR-iBRB2 cells. The Na^+-dependent monocarboxylate transporters SMCT1 and SMCT2 were not expressed in these cells. In conclusion, transfer of nicotinate from blood to retina across the inner BRB occurs primarily via H^+-coupled monocarbxylate transporters.

Keywords

Inner blood-retinal barrier; nicotinic acid; monocarboxylate transporter; Retina; Endothelial cells

Address correspondence and reprint requests to: Vadivel Ganapathy, Ph. D., Department of Biochemistry and Molecular Biology, Medical College of Georgia, Georgia Health Sciences University, Augusta, Georgia, USA (vganapat@georgiahealth.edu), Ken-ichi Hosoya, Ph. D., Graduate School of Medicine and Pharmaceutical Sciences, University of Toyama, Toyama 930-0194, Japan. (hosoyak@pha.u-toyoma.ac.jp).

Introduction

Nicotinic acid (niacin, vitamin B_3) is a biosynthetic precursor of the coenzymes such as nicotinamide adenine dinucleotide (NAD) and nicotinamide adenine dinucleotide phosphate (NADP) (Henderson, 1983), which are indispensable for a multitude of the catabolic and anabolic processes. It is an essential dietary constituent and is readily absorbed from the intestinal tract (Bechgaard and Jespersen, 1977; Sadoogh-Abasian and Evered, 1980). Since the whole body autoradiogram after intravenous administration of [^{3}H]-nicotinic acid in mice shows the presence of radioactivity in the eye as early as 5 min after injection (Carlson and Hanngren, 1964), it is conceivable that nicotinic acid is supplied to the retina from the circulating blood after its absorption in intestinal tract.

Nicotinic acid is also an important therapeutic agent widely used as a lipid-lowering drug and in the treatment of atherosclerotic cardiovascular disease (Bodor and Offermanns, 2008; Carlson, 2005). This effect however requires pharmacological doses. Interestingly, the function of nicotinic acid as a lipid-lowering agent is independent of the role of this vitamin as a constituent of the coenzymes NAD and NADP; instead, this function is mediated through the G-protein-coupled receptor GPR109A to which nicotinic acid serves as a high-affinity agonist (Bodor and Offermanns, 2008). However, chronic use of nicotinic acid at high doses is linked to an ocular complication known as a niacin maculopathy (Gass, 2003; Jampol, 1988; Millay et al., 1988). Because the high-dose administration of nicotinic acid increases its blood concentration (Offermanns, 2006), the abnormal accumulation of nicotinic acid in the retina may contribute to niacin maculopathy. Thus, nicotinic acid is an essential nutrient for maintenance of visual function, but it also produces detrimental effects on the retina at high doses. Therefore, understanding the mechanism of the blood-to-retina transport process of nicotinic acid has biological as well as therapeutic significance. Such knowledge may help in the rational design of a nicotinate dosage regimen for the retinal supplementation of nicotinate and in the treatment of hyperlipidemia without causing the undesirable maculopathy as a side effect.

The nutrient supply to the retina from the circulating blood is regulated by a variety of transporters expressed at the blood-retinal barrier (BRB). The BRB is formed by complex tight junctions of retinal capillary endothelial cells (inner BRB) and retinal pigment epithelial cells (RPE, outer BRB) (Hosoya and Tachikawa, 2009). Since nicotinic acid is a weak electrolyte having a monocarboxylic acid group with a pKa of 4.9, it exists predominantly in the form of a monocarboxylate anion (nicotinate) under physiological conditions. Monocarboxylate transporter 1 (MCT1/solute carrier SLC16A1), a member of the monocarboxylate transporter gene family, transports nicotinate via an electroneutral process, involving co-transport of nicotinate with one H^+ (Simanjuntak et al., 1990; Takanaga et al., 1996). This is a low-affinity process with the Michaelis constant in millimolar range. Sodium-coupled monocarboxylate transporter 1 (SMCT1/SLC5A8), a member of the Na^+/glucose co-transporter gene family, also mediates nicotinate transport, but the process is electrogenic, involving co-transport of nicotinate with 2 Na^+ (Gopal et al., 2005). However, in contrast to transport via MCT1, the transport of nicotinate via SMCT1 is a high-affinity process with the Michaelis constant of 230 μM (Gopal et al., 2007).

Retina must have an optimal supply of nicotinate for its essential metabolic functions. However, there have been no studies reported in the literature on the delivery of nicotinate from the circulation into retina. The purpose of the present study was to investigate the blood-to-retina transport of nicotinate across the inner BRB. *In vivo* transport of nicotinate from the circulating blood to the retina was elucidated using the carotid artery injection technique (Hosoya et al., 2010). The characteristics of nicotinate transport at the inner BRB were examined using a conditionally immortalized rat retinal capillary endothelial cell line

(TR-iBRB2 cells) as an *in vitro* model of inner BRB (Hosoya and Tachikawa, 2009; Hosoya et al., 2001b). The expression of MCTs and SMCTs in TR-iBRB2 cells was investigated by reverse transcription-polymerase chain reaction (RT-PCR). These studies showed for the first time that the transfer of nicotinate across the inner BRB occurs primarily via a low-affinity process involving the H^+-coupled monocarboxylate transporters expressed in the retinal vascular endothelial cells.

Materials and methods

Animals

Male Wistar rats, weighing 160–200 g, were purchased from Harlan Sprague Dawley (Frederick, MD, USA) and Nippon SLC (Hamamatsu, Japan). The investigations using rats described in this report conformed to the guidelines provided in the ARVO Statement on the Use of Animals in Ophthalmic and Vision Research and were approved by the Animal Use and Care Committees in the respective institutions (Georgia Health Sciences University, USA, and the University of Toyama, Japan).

Reagents

[5,6-^{3}H]-Nicotinic acid (60 Ci/mmol) and n-[1-^{14}C]-butanol (2 mCi/mmol) were purchased from American Radiolabeled Chemicals (St. Louis, MO, USA). [^{14}C(U)]-Sucrose (498 mCi/mmol) was obtained Perkin-Elmer Life and Analytical Sciences (Boston, MA, USA). All other chemicals were commercial products of analytical grade.

In vivo blood-to-retina transport of nicotinate

The *in vivo* blood-to-retina transport of nicotinate was evaluated by the carotid injection technique (Alm and Törnquist, 1981; Hosoya et al., 2010). Briefly, rats were anesthetized with an intraperitoneal injection of pentobarbital and then 200 μL of injection solution was injected into the common carotid artery. The injection solution consisted of Ringer-Hepes buffer (141 mM NaCl, 4 mM KCl, 2.8 mM $CaCl_2$, 10 mM Hepes, pH 7.4) which contained a mixture of 6 μCi [^{3}H]-nicotinate, a test compound, and 1 μCi [^{14}C]-sucrose used as a BRB impermeable vascular space marker, or 0.15 μCi [^{14}C]-n-butanol used as a freely diffusible internal reference, in the presence or absence of inhibitors. Rats were decapitated 15 sec after injection, and the retinas and the brains were removed. The retinas were dissolved in 2 N NaOH and subsequently neutralized with 2 N HCl. The radioactivity was measured in a liquid scintillation counter (LSC-5000, Aloka, Tokyo, Japan).

[^{3}H]-Nicotinate uptake by the retina and brain, relative to vascular [^{14}C]-sucrose space, was expressed as following equation (1).

$$\begin{aligned}&\text{Percentage of } [^3\text{H}]-\text{nicotinate uptake}\\&\quad /\text{vascular } [^{14}\text{C}]\\&\quad -\text{sucrose space}\\&\quad =([^3\text{H}]/[^{14}\text{C}](\text{dpm in the retina or brain}))/([^3\text{H}]\\&\quad /[^{14}\text{C}](\text{dpm in the injection solution})) \times 100\end{aligned} \quad (1)$$

[^{3}H]-Nicotinate uptake by the retina, relative to [^{14}C]-n-butanol, a highly diffusible internal reference, was expressed as a retinal uptake index (RUI) according to equation (2). RUI value expresses the fractional uptake of the [^{3}H]-nicotinate as a percentage of the fractional uptake of the reference compound [^{14}C]-n-butanol in the retina.

$$\mathrm{RUI}=([^3\mathrm{H}]/[^{14}\mathrm{C}](\mathrm{dpm\ in\ the\ retina}))/([^3\mathrm{H}]/[^{14}\mathrm{C}](\mathrm{dpm\ in\ the\ injection\ solution}))\times 100 \quad (2)$$

Nicotinate uptake in TR-iBRB2 cells

TR-iBRB2 cells were grown routinely in collagen (type I)-coated tissue culture flasks (BD Biosciences, Bedford, MA, USA) at 33°C under 5% CO_2/air. The permissive-temperature for TR-iBRB2 cells in culture is 33 °C due to the expression of temperature-sensitive large T-antigen (Hosoya et al., 2001b). The culture medium consisted of Dulbecco's modified Eagle's medium (DMEM, Nissui Pharmaceutical Co., Tokyo, Japan) supplemented with 20 mM sodium bicarbonate, 100 U/ml benzylpenicillin potassium, 100 μg/ml streptomycin sulfate, and 10% FBS. For the uptake studies, cells between passages 27 and 32 were used. TR-iBRB2 cells (1×10^5 cells/cm^2) were cultured at 33°C for 48 h on rat tail collagen (type I)-coated 24 well plates (BD Biosciences). After removal of culture medium, cells were washed with extracellular fluid (ECF) buffer, consisting of 122 mM NaCl, 25 mM $NaHCO_3$, 3 mM KCl, 1.4 mM $CaCl_2$, 1.2 mM $MgSO_4$, 0.4 mM K_2HPO_4, 10 mM D-glucose, and 10 mM Hepes (pH 7.4). Uptake was initiated by applying 200 μL ECF-buffer containing 0.2 μCi [^{3}H]-nicotinate (16.7 nM) at 37°C in the presence or absence of inhibitors. Na^+- and Cl^--free uptake buffers were prepared by replacement with equimolar choline chloride and sodium gluconate, respectively. Uptake measurements were performed at 37°C. After a predetermined time period, uptake was terminated by suctioning off the applied solution and immersing the cells in ice-cold ECF-buffer (pH 7.4). The cells were then solubilized in 1 N NaOH and subsequently neutralized with 1 N HCl. The cell-associated radioactivity and protein content were assayed by liquid scintillation counting (LSC-500, Aloka) and detergent compatible protein assay (a DC protein assay kit, Bio-Rad, Hercules, CA, U.S.A.) with bovine serum albumin as a standard.

For kinetic studies, the Michaelis constant (K_t) and the maximal velocity (V_{max}) of nicotinate uptake were calculated from the following equation (3) using the nonlinear least-square regression analysis program, MULTI (Yamaoka et al., 1986).

$$V=V_{max} \times [S]/(K_t+[S]) \quad (3)$$

where V is the nicotinate uptake rate, and S is the nicotinate concentration.

RT-PCR analysis

Total cellular RNA was prepared from phosphate-buffered saline (PBS)-washed cells using an RNeasy Mini Kit (Qiagen, Hilden, Germany). Single-strand cDNA was made from 1 μg total RNA by reverse transcription (RT) using oligo dT primer. The polymerase chain reaction (PCR) was performed using a gene amplification system (GeneAmp PCR system 9700; PE-Applied Biosystems, Foster City, CA, USA) with specific primers for rat MCT1, MCT2, MCT3, MCT4, SMCT1 and SMCT2 (Table 1) through 30 cycles of 94°C for 30 s, 60°C for 1 min, and 72°C for 1 min. The PCR products were separated by electrophoresis on an agarose gel in the presence of ethidium bromide and visualized under ultraviolet light. The molecular identity of the resultant products was confirmed by sequence analysis using a DNA sequencer (ABI PRISM 310; PE-Applied Biosystems).

Data analysis

All data represent means ± S. E. except for kinetic parameters. The data for the kinetic parameters represent means ± S.D. An unpaired, two-tailed Student's *t*-test was used to determine the significance of differences between two groups. Statistical significance of differences among means of several groups was determined by one-way analysis of variance followed by the modified Fisher's least-squares difference method. A p value <0.05 was taken as statistically significant.

Results

In vivo blood-to-retina transport of [^{3}H]-nicotinate

The *in vivo* blood-to-retina influx transport of nicotinate across the BRB was evaluated by the carotid artery injection of [^{3}H]-nicotinate in rats. The [^{3}H]-nicotinate uptake by the retina and brain was 5.4- and 1.9-fold greater, respectively, than that of [^{14}C]-sucrose, a marker for vascular space (Table 2). This could exclude the possibility that the greater activity of retinal [^{3}H]-nicotinate transfer is due to the difference of vascular space in the brain and retina. Unlabeled nicotinate and salicylate, each at a concentration of 20 mM, significantly decreased the retinal uptake of [^{3}H]-nicotinate (52% and 28%, respectively) (Table 3). These results support the conclusion that the BRB possesses specific carrier-mediated transport mechanism(s) for the blood-to-retina transport of nicotinate.

Characteristics of [^{3}H]-nicotinate uptake by TR-iBRB2 cells

To investigate the mechanism(s) of the blood-to-retina transport of nicotinate at the inner BRB, TR-iBRB2 cells, a rat *in vitro* model of inner BRB (Hosoya et al., 2001b), were used. The effect of extracellular pH on [^{3}H]-nicotinate uptake by TR-iBRB2 cells was examined over the pH range 5.0 to 7.4 (Fig. 1A). The [^{3}H]-nicotinate uptake was markedly stimulated when the extracellular pH was changed from 7.4 to 5.0. The [^{3}H]-nicotinate uptake at pH 5.0 and 6.0 was 16.4- and 3-fold greater, respectively, than that at pH 7.4. In the presence of 10 mM unlabeled nicotinate, the [^{3}H]-nicotinate uptake at pH 5.0, 6.0, and 7.4 was significantly inhibited by 82%, 69%, and 60%, respectively. The [^{3}H]-nicotinate uptake at pH 6.0 and 7.4 exhibited a linear time-dependent increase for up to 3 min (Fig. 1B). The initial uptake rate of [^{3}H]-nicotinate at pH 6.0 [0.126 pmol/(min·mg protein)] was 4.6-fold greater than that at pH 7.4 [0.0275 pmol/(min·mg protein)]. Replacement of Na^+ with choline in the uptake buffer reduced the uptake at pH 7.4 by 10% although it had no effect on the [^{3}H]-nicotinate uptake at pH 6.0 (Table 4). The absence of Cl^- did not reduce the [^{3}H]-nicotinate uptake both at pH 6.0 and 7.4 (Table 4). These results suggest that the [^{3}H]-nicotinate uptake in these cells involves pH-dependent and mostly Na^+-independent carrier-mediated process. Subsequent uptake experiments were performed at pH 6.0 to characterize the nicotinate transport. As shown in Fig. 2, [^{3}H]-nicotinate uptake by TR-iBRB2 cells at pH 6.0 exhibited saturable kinetics with a K_t of 7.0 ± 1.0 mM and a V_{max} of 21.2 ± 1.5 nmol/(min·mg protein), respectively. The inhibitory effects of various compounds on [^{3}H]-nicotinate uptake were examined (Table 5). Endogenous monocarboxylic acids such as L-lactate and pyruvate, and monocarboxylic drugs such as valproate, salicylate and ibuprofen significantly inhibited the uptake by more than 33%. In contrast, L-phenylalanine had no effect on the [^{3}H]-nicotinate uptake. These results suggest that the [^{3}H]-nicotinate uptake in TR-iBRB2 cells is mostly likely mediated by the H^+-coupled monocarboxylate transporters belonging to the MCT gene family.

Expression of MCTs and SMCTs mRNAs in TR-iBRB2 cells

The MCT family consists of 14 members, of which only the first four isoforms (MCT1–MCT4) have been functionally characterized as H^+-coupled monocarboxylate transporters

(Halestrap and Meredith, 2004; Halestrap and Price, 1999). To determine the expression of MCT1–4 and SMCT1–2 in TR-iBRB2 cells, RT-PCR analysis was performed. The bands corresponding to the expected size (Table 1) for MCT1, MCT2 and MCT4 were amplified from TR-iBRB2 cells as well as tissues used as a positive control (Fig. 3). The nucleotide sequences of these products were identical to those of rat MCT1, MCT2, and MCT4, respectively, reported in the GenBank. There was no evidence for the expression of SMCT1 and SMCT2 in these cells. These results indicate that MCT1, MCT2, and MCT4 are expressed in TR-iBRB2 cells whereas MCT3, SMCT1, and SMCT2 mRNAs are not. This expression pattern of the monocarboxylate transporters corroborate the uptake data which showed that the uptake of nicotinate in these cells occurred predominantly via Na^+-independent, H^+-coupled uptake process, suggesting involvement of transporters belonging to the MCT family.

Discussion

The present study demonstrates that nicotinate is supplied from the circulating blood to the retina via a carrier-mediated process at the BRB. The characteristics of nicotinate uptake by TR-iBRB2 cells indicate that H^+-coupled MCTs are involved in nicotinate transport at the inner BRB.

In vivo studies reveal that the blood-to-retina transport activity of nicotinate is 3-fold greater than the blood-to-brain transport (Table 2). The retina-predominant accumulation of nicotinate is evidenced by the [^{3}H]nicotinate autoradiogram at 5 min after its intravenous injection, in which the intense signals were detected in the eye but not in the brain (Carlson and Hanngren, 1964). The greater activity of nicotinate transfer at the BRB is also true of the L-lactate transfer since the retinal uptake index value of L-lactate (69.6%) is greater than the brain uptake index value (18.7%) (Alm and Törnquist, 1985). This implies that a developed transport system for monocarboxylates is present at the BRB. The *in vivo* [^{3}H]nicotinate uptake by the retina is significantly inhibited by unlabeled nicotinate and salicylate each at a concentration of 20 mM which is approximately 3-fold greater than a Kt value of nicotinate uptake by TR-iBRB2 cells (Fig. 2). This evidence supports the conclusion that a saturable and carrier-mediated transport process specific for monocarboxylates is involved in the supply of nicotinate to the retina. The incomplete inhibition is presumably due to the dilution of injected unlabeled nicotinate and salicylate in the circulating blood and/or the contribution of passive diffusion process of the retinal nitocinate transfer. Although the *in vivo* transport activity of nicotinate reflects the functions of both the inner and outer BRBs, the presence of nicotinate transport at the inner BRB is strongly suggested by the fact that nicotinate uptake occurs in TR-iBRB2 cells. TR-iBRB2 cells take up nicotinate via an H^+-dependent carrier-mediated transport process rather than by passive diffusion in accordance with the pH-partition theory (Brodie and Hogben, 1957). The nicotinate uptake was concentration-dependent and saturable with a K_t value of 7 mM (Fig. 2). This value for Michaelis constant is comparable to the corresponding value reported in the literature for H^+-coupled and Na^+-independent nicotinate uptake by primary cultures of astrocytes (2.8 mM; Shimada et al., 2006). Monocarboxylates such as L-lactate, salicylate, valproate, pyruvate, and ibuprofen inhibited nicotinate uptake by TR-iBRB2 cells by 35–65% whereas the amino acid L-phenyalanine had no effect (Table 5). The absence of Na^+ inhibited the nicotinate uptake by 10% at pH 7.4 (Table 4), suggesting minimal contribution of Na^+-dependent transport processes to the observed uptake in TR-iBRB2 cells. We have reported that an inward H^+ gradient for L-lactate transport in TR-iBRB2 cells appears to be generated by Na^+/H^+ exchanger (NHE) (Hosoya et al., 2001a). In this regard, the small decrease in nicotinate uptake by TR-iBRB2 cells under Na^+-free conditions may be due to a reduction of inward H^+ gradient as the driving force under these conditions. This notion is supported by the data indicating that SMCT1 and SMCT2 mRNAs are not

expressed in TR-iBRB2 cells (Fig. 3). These characteristics suggest that nicotinate uptake by TR-iBRB2 cells is mediated by H^+-coupled MCT(s) under physiological conditions. [^{3}H]Nicotinate uptake by TR-iBRB2 cells was increased under Cl^--free conditions (Table 4). Yabuuchi et al. (1998) have reported that an anion exchanger (AE) 2 mediates nicotinate uptake as an antiport of outward Cl^- and inward nicotinate under Cl^--free conditions. Although it remains unknown which subtype of anion exchanger is expressed in the retinal capillary endothelial cells, an anion exchanger would be involved in the enhancement of nicotinate uptake by TR-iBRB2 cells in Cl^--free buffer. However, this type of anion exchange seems unlikely under physiological conditions.

RT-PCR analysis reveals that MCT1, MCT2, and MCT4 mRNAs are detected in TR-iBRB2 cells (Fig. 3). Gerhart et al. (1999) used the immunohistochemical method to show that MCT1 is localized on the luminal and abluminal plasma membranes of retinal endothelial cells and that MCT2 is not expressed in these cells. The exact localization of MCT4 in retinal endothelial cells is not known. Based on our data, we conclude that a H^+-coupled monocarbxylate transporter, most probably MCT1, at the inner BRB is responsible for the supply of nicotinate to the retina from the blood circulation. Considering that MCT1 protein is abundantly expressed in brain capillary endothelial cells (Kamiie et al., 2008), one possible explanation for the greater activity of the blood-to-retina nicotinate transfer is the difference of the protein amount of MCTs expressed in brain and retinal capillary endothelial cells. It is thus intriguing to quantify the MCT proteins at inner BRB by means of the absolute quantification method developed by Kamiie et al. (2008). Another possibility is that the outer BRB as well as inner BRB contribute to the vectorial transfer of nutrients in the blood-to-retina direction (Hosoya and Tachikawa, 2009). It has been reported that SMCT1 is localized on the basolateral membrane of RPE cells and mediates Na^+-dependent nicotinate uptake (Martin et al., 2007). H^+-coupled MCT3 is also located exclusively on the basolateral membrane of RPE cells (Philp et al., 1998). The MCTs and SMCT1 at the inner and outer BRBs contribute to nicotinate delivery to the retina *in vivo*.

The K_t value of 7 mM for nicotinate transport in TR-iBRB2 cells (Fig. 2) is far greater than the plasma level of nicotinate (100–400 nM; Offermanns, 2006). The plasma concentration of L-lactate is 1 mM (Buchalter et al., 1989), which is close to the K_t value for L-lactate uptake by TR-iBRB2 cells (1.66 mM; Hosoya et al., 2001a). Thus, the blood-to-retina transport of nicotinate across the inner and outer BRBs could not be completely saturated by endogenous monocarboxylates. In this regard, the rate of retinal nitotinate transport seems to depend on the blood concentration of nitotinate. High doses of nicotinate are clinically used as an antidyslipidemic drug to decrease low-density lipoprotein cholesterol levels and increase high-density lipoprotein choresterol levels (Carlson, 2005). Total daily dose of nicotinate are usually 1.5–3.0 g, resulting in peak plasma concentration of 50–300 μM (Offermanns, 2006). Because this blood concentration is still much smaller than the K_t value of nicotinate uptake by TR-iBRB2 cells, the blood-to-retina transport of nicotinate during nicotinate drug therapy is estimated to be approximately 1000-fold greater than that under normal physiological conditions. It has been reported that chronic use of nicotinate at high does is associated with several side effects, including an ocular complication known as niacin maculopathy (Davis et al., 2008). The characteristics of nicotinate transport at the inner BRB may provide at least a partial explanation for this adverse effect: the elevated concentration of nicotinate in the circulating blood causes the increased entry of nicotinate into the retina. How elevated levels of nicotinate in the retina causes maculopathy remains to be determined.

In conclusion, this is the first study to demonstrate that H^+-coupled monocarbxylate transporter, most likely MCT1, functions as a supplying pathway for nicotinate as an indispensable vitamin from the circulating blood to the retina across the inner BRB. These

findings may assist in the design of a suitable nicotinate dosage regimen to prevent the abnormal accumulation of nicotinate used as an antidislipidemic drug.

Highlights

Nicotinic acid is a constituent of the coenzymes NAD and NADP. Nicotinic acid is widely used at high doses as a lipid-lowering drug. We examined [^{3}H]nicotinate transport to the retina across the inner BRB. [^{3}H]Nicotinate transport to the retina is mediated by MCTs at the inner BRB. Information will assist in the design of a suitable nicotinate dosage regimen.

Acknowledgments

We would like to thank S. Akanuma for technical assistance. This study was supported, in part, by the National Institutes of Health Grant EY018053 and the Grant-in-Aid for Scientific Research from the Ministry of Education, Science, Sports, and Culture, and from the Japan Society for the Promotion of Science, Japan.

References

Alm A, Törnquist P. The uptake index method applied to studies on the blood-retinal barrier. I. A methodological study. Acta Physiol Scand. 1981; 113:73–79. [PubMed: 7315440]

Alm A, Törnquist P. Lactate transport through the blood-retinal and the blood-brain barrier in rats. Ophthalmic Res. 1985; 17:181–184. [PubMed: 4011131]

Bechgaard H, Jespersen S. GI absorption of niacin in humans. J Pharm Sci. 1977; 66:871–872. [PubMed: 874791]

Bodor ET, Offermanns S. Nicotinic acid: an old drug with a promising future. Br J Pharmacol. 2008; 153 Suppl 1:S68–S75. [PubMed: 18037924]

Brodie BB, Hogben CA. Some physico-chemical factors in drug action. J Pharm Pharmacol. 1957; 9:345–380. [PubMed: 13439526]

Buchalter SE, et al. Regulation of lactate metabolism in vivo. Diabetes Metab Rev. 1989; 5:379–391. [PubMed: 2656161]

Carlson LA. Nicotinic acid: the broad-spectrum lipid drug. A 50th anniversary review. J Intern Med. 2005; 258:94–114. [PubMed: 16018787]

Carlson LA, Hanngren A. Initial distribution in mice of ^{3}H-labeled nicotinic acid studied with autoradiography. Life Sci. 1964; 3:867–871. [PubMed: 14201696]

Davis MJ, et al. Diagnostic and therapeutic challenges. Retina. 2008; 28:520–524. [PubMed: 18327149]

Gass JD. Nicotinic acid maculopathy. 1973. Retina. 2003; 23:500–510. [PubMed: 15035390]

Gerhart DZ, et al. Distribution of monocarboxylate transporters MCT1 and MCT2 in rat retina. Neuroscience. 1999; 92:367–375. [PubMed: 10392858]

Gopal E, et al. Sodium-coupled and electrogenic transport of B-complex vitamin nicotinic acid by slc5a8, a member of the Na/glucose co-transporter gene family. Biochem J. 2005; 388:309–316. [PubMed: 15651982]

Gopal E, et al. Transport of nicotinate and structurally related compounds by human SMCT1 (SLC5A8) and its relevance to drug transport in the mammalian intestinal tract. Pharm Res. 2007; 24:575–584. [PubMed: 17245649]

Halestrap AP, Meredith D. The SLC16 gene family-from monocarboxylate transporters (MCTs) to aromatic amino acid transporters and beyond. Pflugers Arch. 2004; 447:619–628. [PubMed: 12739169]

Halestrap AP, Price NT. The proton-linked monocarboxylate transporter (MCT) family: structure, function and regulation. Biochem J. 1999; 343(Pt 2):281–299. [PubMed: 10510291]

Henderson LM. Niacin. Annu Rev Nutr. 1983; 3:289–307. [PubMed: 6357238]

Hosoya K, et al. MCT1-mediated transport of L-lactic acid at the inner blood-retinal barrier: a possible route for delivery of monocarboxylic acid drugs to the retina. Pharm Res. 2001a; 18:1669–1676. [PubMed: 11785685]

Hosoya K, Tachikawa M. Inner blood-retinal barrier transporters: role of retinal drug delivery. Pharm Res. 2009; 26:2055–2065. [PubMed: 19568694]

Hosoya K, et al. Conditionally immortalized retinal capillary endothelial cell lines (TR-iBRB) expressing differentiated endothelial cell functions derived from a transgenic rat. Exp Eye Res. 2001b; 72:163–172. [PubMed: 11161732]

Hosoya K, et al. Lipophilicity and transporter influence on blood-retinal barrier permeability: a comparison with blood-brain barrier permeability. Pharm Res. 2010; 27:2715–2724. [PubMed: 20859661]

Jampol LM. Niacin maculopathy. Ophthalmology. 1988; 95:1704–1705. [PubMed: 3231439]

Kamiie J, et al. Quantitative atlas of membrane transporter proteins: development and application of a highly sensitive simultaneous LC/MS/MS method combined with novel in-silico peptide selection criteria. Pharm Res. 2008; 25:1469–1483. [PubMed: 18219561]

Martin PM, et al. Expression of the sodium-coupled monocarboxylate transporters SMCT1 (SLC5A8) and SMCT2 (SLC5A12) in retina. Invest Ophthalmol Vis Sci. 2007; 48:3356–3363. [PubMed: 17591909]

Millay RH, et al. Niacin maculopathy. Ophthalmology. 1988; 95:930–936. [PubMed: 3174043]

Offermanns S. The nicotinic acid receptor GPR109A (HM74A or PUMA-G) as a new therapeutic target. Trends Pharmacol Sci. 2006; 27:384–390. [PubMed: 16766048]

Philp NJ, et al. Monocarboxylate transporter MCT1 is located in the apical membrane and MCT3 in the basal membrane of rat RPE. Am J Physiol. 1998; 274:R1824–R1828. [PubMed: 9841555]

Sadoogh-Abasian F, Evered DF. Absorption of nicotinic acid and nicotinamide from rat small intestine in vitro. Biochim Biophys Acta. 1980; 598:385–391. [PubMed: 6445756]

Shimada A, et al. Functional characteristics of H^+-dependent nicotinate transport in primary cultures of astrocytes from rat cerebral cortex. Neurosci Lett. 2006; 392:207–212. [PubMed: 16213084]

Simanjuntak MT, et al. Carrier-mediated uptake of nicotinic acid by rat intestinal brush-border membrane vesicles and relation to monocarboxylic acid transport. J Pharmacobiodyn. 1990; 13:301–309. [PubMed: 2273446]

Takanaga H, et al. Nicotinic acid transport mediated by pH-dependent anion antiporter and proton cotransporter in rabbit intestinal brush-border membrane. J Pharm Pharmacol. 1996; 48:1073–1077. [PubMed: 8953511]

Yabuuchi H, et al. Possible role of anion exchanger AE2 as the intestinal monocarboxylic acid/anion antiporter. Pharm Res. 1998; 15:411–416. [PubMed: 9563070]

Yamaoka K, et al. An analysis program MULTI(ELS) based on extended nonlinear least squares method for microcomputers. J Pharmacobiodyn. 1986; 9:161–173. [PubMed: 3754893]

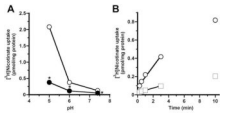

Figure 1.

pH-dependence of [^{3}H]-nicotinate uptake by TR-iBRB2 cells. (A) [^{3}H]-Nicotinate (16.7 nM) uptake at pH 5.0, 6.0, and 7.4 was measured in the absence (open circle) or presence (closed circle) of 10 mM nicotinate for 3 min at 37°C. Each point represents the mean ± S. E. (n = 4). *p<0.01 significantly different from the uptake in the absence of 10 mM nicotinate. (B) Time-course of [^{3}H]-nicotinate uptake by TR-iBRB2 cells at pH 6.0 (open circle) and 7.4 (open square). [^{3}H]-Nicotinate (16.7 nM) uptake was measured at the indicated time at 37 °C. Each point represents the mean ± S. E. (n = 4).

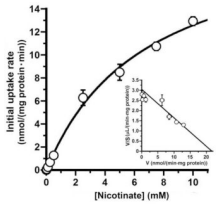

Figure 2.

Concentration-dependence of nicotinate uptake by TR-iBRB2 cells. Nicotinate uptake was measured for 3 min at 37°C and pH 6.0 with increasing concentrations of nicotinate. [^{3}H]-Nicotinate (16.7 nM) was present in all uptake measurements as the tracer, and the concentration of nicotinate was varied using unlabeled nicotinate. Each point represents the mean ± S. E. (n = 4). Inset: Eadie-Scatchard plot exhibiting a single saturable uptake process.

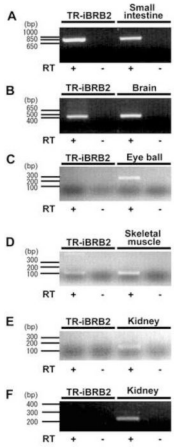

Figure 3.
RT-PCR analysis of rat MCT1 (A), MCT2 (B), MCT3 (C), MCT4 (D), SMCT1 (E), SMCT2 (F) in TR-iBRB2 cells. “+” and “−” indicate RT (+) and RT (−), respectively.

Table 1

Oligonucleotide primers used for PCR amplification of cDNAs

Target mRNA	Accession number	Upstream primer (5'to 3')	Downstream primer (5'to 3')	Product size (bp)
MCT1 (SLC16A1)	NM_012716	gaaaaactcaagtccaaagagtct	tttcattgtcttcttgggcttct	801
MCT2 (SLC6A7)	U62316	cctctgccccctagcccatt	tctgagggaggattgtgtgtatt	447
MCT3 (SLC16A8)	NM_031744	tcaagcgcgacttcggggcaggtta	ccagcatgatgagcgacggctggaa	267
MCT4 (SLC16A3)	NM_030834	tcaggaggcaagctgctggacgcaa	agttgcccagcagcagcacaaggga	103
SMCT1 (SLC5A8)	XM_576209	tcggcggccatcggcatctattacg	acagcggacatgaagctggcggtga	134
SMCT2 (SLC5A12)	NM_001108588	catggcatgtgtggtggaccgatgc	cacaggcctgctggaaagctggtaggct	246

Table 2

Comparison of *in vivo* [^{3}H]-nicotinate uptake by the retina and brain

	[^{3}H]-Nicotinate uptake/[^{14}C]-sucrose space (%)
Retina	540±52
Brain	185±31

[^{3}H]-Nicotinate (6 μCi/head), and a vascular space marker, [^{14}C]-sucrose (1 μCi/head), were injected into the common carotid artery. Each value represents the mean ± S. E. (n = 4).

Table 3

Effect of unlabeled nicotinate and salicylate on *in vivo* retinal uptake of [^{3}H]-nicotinate in rats

Inhibitors	Retinal uptake index (%)	% of control
Control	105 ± 10	100 ± 10
Nicotinate	50.2 ± 4.7*	47.9 ± 4.4*
Salicylate	75.1 ± 2.4**	71.6 ± 2.3**

[^{3}H]-Nicotinate (6 μCi/head), and a reference compound, [^{14}C]-n-butanol (0.15 μCi/head), were injected into the common carotid artery in the absence or presence of 20 mM inhibitors. Each value represents the mean ± S. E. (n = 3–6).

* $p<0.01$,

** $p<0.05$ significantly different from control.

Table 4

Na^+- and Cl^--dependence on [^{3}H]-nicotinate uptake by TR-iBRB2 cells

Conditions	% of control
pH=7.4	
Control	100 ± 2
Na^+-free	89.9 ± 4.2**
Cl^--free	153 ± 2*
pH=6.0	
Control	100 ± 6
Na^+-free	109 ± 3
Cl^--free	239 ± 8*

[^{3}H]-Nicotinate uptake (16.7 nM) by TR-iBRB2 cells was measured at 37 °C for 3 min in the presence (control) or absence of Na^+ and Cl^-. Each value represents the mean ± S. E. (n = 3–4).

* $p<0.01$,

** $p<0.05$, significantly different from control.

Table 5

Inhibitory effect of monocarboxylates on [^{3}H]-nicotinate uptake by TR-iBRB2 cells

Inhibitors	% of control
Control	100 ± 4
L-Lactate	55.2 ± 1.4*
Salicylate	35.2 ± 1.3*
Valproate	39.5 ± 1.8*
Pyruvate	43.4 ± 2.9*
Ibuprofen	65.5 ± 1.6*
L-Phenylalanine	97.4 ± 2.4

[^{3}H]-Nicotinate uptake (16.7 nM) by TR-iBRB2 cells was measured at 37°C and pH 6.0 for 3 min in the absence (control) and presence of inhibitors, each at a concentration of 10 mM except for ibuprofen (500 μM). Each value represents the mean ± S. E. (n = 3–4).

* $p<0.01$, significantly different from control.